Constrained variational calculations for many-body spin-polarized atomic deuterium

1999 J. Phys.: Condens. Matter 11 8017

(http://iopscience.iop.org/0953-8984/11/41/306)

J. Phys.: Condens. Matter **11** (1999) 8017–8034. Printed in the UK PII: S0953-8984(99)04515-4

Constrained variational calculations for many-body spin-polarized atomic deuterium

B Skjetne and E Østgaard

The Institute of Physics, Lade, Norwegian University of Science and Technology, N-7034 Trondheim, Norway

Received 24 May 1999, in final form 12 August 1999

Abstract. A lowest-order constrained variational (LOCV) method, with modified conditions of healing on the two-body Jastrow wave function, is investigated in calculations for the ground-state energy levels of many-body spin-polarized atomic deuterium. Results are obtained for the $\downarrow D_1^{\uparrow}$, $\downarrow D_2^{\uparrow}$ and $\downarrow D_3^{\uparrow}$ phases, corresponding to equal occupations of one, two or three nuclear spin states. Estimates for the optimum healing conditions are obtained by comparison of LOCV results with current Monte Carlo benchmarks. The nature of the phases, i.e., quantum gas or quantum liquid, is discussed, the energy of the $\downarrow D_1^{\uparrow}$ phase in our calculations always occurring above the gas–liquid interphase for healing conditions within a physically acceptable range.

1. Introduction

The helium liquids have long been a favourite testing ground for many-body methods in quantum physics. In recent years an increasing amount of attention has been directed towards spin-polarized quantum systems, notably liquid ^{3}He. Some systems, however, such as electron-spin-polarized atomic hydrogen, will exhibit properties with a quantum behaviour even more extreme than that observed in liquid ^{3}He. This can be visualized using the 'quantum parameter', i.e., $\eta = \hbar^2/(m\epsilon\sigma^2)$, where ϵ and σ are related to the depth and repulsive core range, respectively, of the two-body interaction [1]. Aggregates of weakly interacting elements of low mass should then be strongly influenced by quantum mechanics, the lightest element being hydrogen. The alignment of electron spins to prevent the formation of diatomic H_2 molecules would then enhance the zero-point energy even more.

Hydrogen exists in the form of three isotopes: hydrogen, deuterium and tritium, commonly denoted as H, D and T, respectively. In many-body calculations, electron-spin-polarized D, or $\downarrow$D, is interesting from several points of view. One is that bulk $\downarrow$D, in the absence of external pressure, should exist close to the gas–liquid interphase. Only small variations in the external pressure or field would then be needed in order to observe critical behaviour near the transition. Hence the role of the nuclear spin, denoted as $D^{\uparrow}$, is important, since the ground-state energy of the bulk system then will depend on how $\downarrow$D atoms are distributed among the spin states available. The deuteron spin being $I = 1$, bulk $\downarrow D^{\uparrow}$ should exhibit three possible levels of degeneracy, since $I_z = +1, 0, -1$. Access to a given state of polarization should then be possible by the controlled application of an external magnetic field. With only one spin state occupied, bulk $\downarrow D_1^{\uparrow}$ would be a one-component Fermi system which resembles spin-polarized liquid ^{3}He, i.e., liquid $^3He_1^{\uparrow}$. Cases of two- and three-component Fermi systems would then

0953-8984/99/418017+18$30.00

be bulk $\downarrow D_2^{\uparrow}$ and $\downarrow D_3^{\uparrow}$, respectively, where the former is analogous to unpolarized ^{3}He, i.e., liquid $^3He_2^{\uparrow}$, and the latter has no such analogue.

Results for the ground-state energy levels of many-body $\downarrow D_1^{\uparrow}$, $\downarrow D_2^{\uparrow}$ and $\downarrow D_3^{\uparrow}$ are here obtained in calculations with a constrained variational approach, which improves upon the basic Jastrow function without going explicitly beyond second order. The modification involves the use of a parameter for the healing condition which is derived from the cluster expansion. In numerical calculations this parameter is adjusted with respect to some known property of the system, such as the equilibrium density. This is somewhat reminiscent of the approach in Landau theory, where a number of parameters are 'tuned' to reproduce certain experimental results. Other properties may in principle then be derived, which might not be experimentally accessible. Whereas Landau theory is of a phenomenological nature, however, the modified LOCV method is closer to the pure microscopic approach. Small-scale variations, which might exist in the density dependence of some physical quantities, should then be easily accessible since there is no stochastic element involved in such calculations. For instance, the polarization dependences of quantities such as the compressibility, sound velocity and magnetic susceptibility are not known in the case of many-body electron-spin-polarized atomic deuterium.

The LOCV method may be used for Bose systems as well as Fermi systems, previous results for liquid ^{4}He [2, 3] being in excellent agreement with Monte Carlo results [4]. In the case of Fermi systems, results for both the unpolarized and fully spin-polarized phases of liquid ^{3}He [5] were also found to be in excellent agreement with variational Monte Carlo (VMC) and Fermi hypernetted-chain (FHNC) results [6, 7]. Our aim in this work, then, has been to determine how well the current benchmark results reported in VMC many-body calculations [8] for $\downarrow D_1^{\uparrow}$, $\downarrow D_2^{\uparrow}$ and $\downarrow D_3^{\uparrow}$ can be reproduced in the constrained variational approach.

Fortunately, the basic two-body hydrogen interaction is very accurately known. A reliable theoretical description is given by the $b^3\Sigma_u^+$ potential, derived by Kolos and Wolniewicz [9] and used by Panoff and Clark in their VMC calculations [8]. It is accurately reproduced by a Silvera model [10, 11], here denoted as S1. A modified form of the S1 model, however, is generally regarded as the best empirical representation of the $b^3\Sigma_u^+$ potential. This model [12] is denoted as S2 in our calculations. To illustrate the response of the results to the choice of interaction, we also include, using the conventional healing condition in LOCV calculations, a few results obtained with both the S1 model and an older Lennard-Jones (LJ) model [1] in addition to results obtained with the S2 model.

2. The LOCV method

In classical statistical mechanics, the many-body problem is developed from the configuration integral

$$Q_N(V,T) = \int \exp\bigl[-\beta U(\boldsymbol{r}_1,\ldots,\boldsymbol{r}_N)\bigr]\,\mathrm{d}^{3N}r_1\,\cdots\,\mathrm{d}^{3N}r_N \tag{1}$$

where $U \equiv U(\boldsymbol{r}_1,\ldots,\boldsymbol{r}_N)$ is the potential energy, i.e.,

$$U = \sum\sum_{1\leqslant i<j\leqslant N} v(\boldsymbol{r}_i,\boldsymbol{r}_j) + \sum\sum_{1\leqslant i<j<k\leqslant N}\sum v(\boldsymbol{r}_i,\boldsymbol{r}_j,\boldsymbol{r}_k) + \cdots.$$

The LOCV method [13] depends on a generalization of Van Kampen's expansion [14] of equation (1) to quantum statistical mechanics, enabling the energy

$$E = \frac{\langle\Psi|H|\Psi\rangle}{\langle\Psi|\Psi\rangle} \tag{2}$$

to be developed in a cluster series. This technique is Nosanow's cluster expansion [15], and requires the use of a generalized normalization integral, given by

$$M(\gamma) = \left\langle \Psi | \mathrm{e}^{\gamma H} | \Psi \right\rangle .$$

An expression for the energy consistent with (2) is then

$$E = \lim_{\gamma \to 0} \frac{\partial}{\partial \gamma} \left[\ln M(\gamma) \right] \tag{3}$$

whereby a series expansion follows by assuming a product expansion for $M(\gamma)$. In Nosanow's method we thus treat the generalized normalization integral in the spirit of Van Kampen's technique. Hence,

$$M(\gamma) = \prod_{n=1}^{N} M_n(\gamma) \tag{4}$$

is obtained, where

$$M_n(\gamma) = \prod_{\{n\} \in N} \left\{ \left\langle \Psi_n | \mathrm{e}^{\gamma H_n} | \Psi_n \right\rangle \left[\prod_{m=1}^{n-1} M_m^{(n)}(\gamma) \right]^{-1} \right\}$$

is expanded with respect to all distinct clusters, Ψ_n representing a cluster wave function. The nth-order term is

$$M_n(\gamma) = \prod_{1 \leqslant i_1 < i_2 \ll i_n \leqslant N} \cdots \prod \frac{\left\langle \Psi(\boldsymbol{x}_{i_1} \boldsymbol{x}_{i_2} \cdots \boldsymbol{x}_{i_n}) | \mathrm{e}^{\gamma H(\boldsymbol{x}_{i_1} \boldsymbol{x}_{i_2} \cdots \boldsymbol{x}_{i_n})} | \Psi(\boldsymbol{x}_{i_1} \boldsymbol{x}_{i_2} \cdots \boldsymbol{x}_{i_n}) \right\rangle}{M_1(\gamma; \boldsymbol{x}_{i_1} \cdots \boldsymbol{x}_{i_n}) \cdots M_{n-1}(\gamma; \boldsymbol{x}_{i_1} \cdots \boldsymbol{x}_{i_n})} \tag{5}$$

where

$$M_1(\gamma; \boldsymbol{x}_{i_1} \cdots \boldsymbol{x}_{i_n}) = \prod_{i_1 \leqslant j_1 \leqslant i_n} \left\langle \Psi(\boldsymbol{x}_{j_1}) | \mathrm{e}^{\gamma H(\,)} | \Psi(\,) \right\rangle$$

$$M_2(\gamma; \boldsymbol{x}_{i_1} \cdots \boldsymbol{x}_{i_n}) = \prod_{i_1 \leqslant j_1 < j_2 \leqslant i_n} \frac{\left\langle \Psi(\boldsymbol{x}_{j_1} \boldsymbol{x}_{j_2}) | \mathrm{e}^{\gamma H(\,)} | \Psi(\,) \right\rangle}{M_1(\,)}$$

$$\vdots$$

$$M_{n-1}(\gamma; \boldsymbol{x}_{i_1} \cdots \boldsymbol{x}_{i_n}) = \prod_{i_1 \leqslant j_1 < j_2 \ll j_{n-1} \leqslant i_n} \cdots \prod \frac{\left\langle \Psi(\boldsymbol{x}_{j_1} \cdots \boldsymbol{x}_{j_{n-1}}) | \mathrm{e}^{\gamma H(\,)} | \Psi(\,) \right\rangle}{M_1(\,) \cdots M_{n-2}(\,)}.$$

Using (3), (4) and (5), the energy contributions can be obtained. Hence, the total ground-state energy is finally obtained as

$$E = \sum_{n=1}^{N} \left\{ \sum \sum_{1 \leqslant i_1 < i_2 \ll i_n \leqslant N} \cdots \sum C_n(i_1, i_2, \ldots, i_n) \right\} \tag{6}$$

where the nth-order term is

$$C_n(i_1, i_2, \ldots, i_n) = \frac{\langle \Psi_n | H_n | \Psi_n \rangle}{\langle \Psi_n | \Psi_n \rangle} - \sum_{m=1}^{n-1} \left\{ \sum_{i_1 \leqslant j_1 \ll j_m \leqslant i_n} \cdots \sum C_m(j_1, j_2, \ldots, j_m) \right\}.$$

Strong repulsion at short separation is the dominant interaction feature. Hence, with $\boldsymbol{x}_i$ representing both orbital and nuclear spin coordinates, a convenient choice of trial wave function for the components of

$$\Psi(\{i, j\}) = \prod_{\{i,j\} \in N} \Psi_2 \equiv \prod \prod_{1 \leqslant i < j \leqslant N} \Psi(\boldsymbol{x}_i, \boldsymbol{x}_j)$$

is the Jastrow function [16], i.e.,

$$\Psi_2 = \frac{1}{\sqrt{\Omega}}\Phi(\boldsymbol{R})\sum_{L=0}^{\infty} f_L(r)\mathcal{P}_L\phi(\boldsymbol{r},\sigma) \tag{7}$$

where the centre-of-mass wave function, using $\boldsymbol{R} = \frac{1}{2}(\boldsymbol{r}_i + \boldsymbol{r}_j)$, reads

$$\Phi(\boldsymbol{R}) = \frac{1}{\sqrt{\Omega}}\exp(\mathrm{i}\boldsymbol{K}\cdot\boldsymbol{R})$$

and $\mathcal{P}_L$ is a projection operator for the Lth partial wave. With $r \equiv |\boldsymbol{r}_i - \boldsymbol{r}_j|$ for the relative coordinate, $f_L(r)$ is a spherically symmetric correlation function. On physical grounds, we require (i) $f_L \to 0$ in the limit of zero separation and (ii) $f_L \to 1$ in the limit of very large separations. In practical calculations, however, it will be convenient to specify some finite value d_L for the interparticle separation, at which correlations vanish. When this condition is realized, the 'wound' in the wave function, as caused by the potential interaction energy, has been 'healed', and consequently d_L is known as the healing distance. Thus, (ii) above should be replaced by

$$f_L(r = d_L) = 1. \tag{8}$$

The physical justification of (8) is the assumption that two-body correlations in the system are mainly due to strong repulsive effects at short, i.e., finite, range. Nevertheless, weaker correlations exist at intermediate ranges which, in turn, means that this condition is not strictly true when $r > d$. The specification of a d_L at which correlations cease altogether, however, requires the additional condition

$$f_L'(r > d_L) = 0$$

which implies that (8) must be extended to separations for which $r > d$. Furthermore, $d_L = d$ is imposed for all L since, due to the finite range of the interaction core, correlations in higher L-states must be weak. Finally, the boundary conditions on $f_L(r)$ are stated as

$$\begin{aligned} &f_L(r = 0) = 0 \\ &f_L(r > d) = 1 \\ &f_L'(r > d) = 0. \end{aligned} \tag{9}$$

Assuming translational invariance, i.e., plane waves for the single-particle wave functions, the uncorrelated relative contribution to (7) reads

$$\phi(\boldsymbol{r},\sigma) = \exp(\mathrm{i}\boldsymbol{k}\cdot\boldsymbol{r})\chi^{(n)}(\sigma_i,\sigma_j) - \exp(-\mathrm{i}\boldsymbol{k}\cdot\boldsymbol{r})\chi^{(n)}(\sigma_j,\sigma_i) \tag{10}$$

where an expansion in terms of partial waves L is used, i.e.,

$$\exp(\pm\mathrm{i}\boldsymbol{k}\cdot\boldsymbol{r}) = \sum_{L=0}^{\infty}(\pm 1)^L \mathrm{i}^L(2L+1)j_L(kr)P_L(\cos\theta).$$

In the case of spin-1 deuterons, the distinct permutations of σ_i, σ_j on χ_i, χ_j result in nine nuclear spin states; that is,

$$\chi^{(n)}(\sigma_i,\sigma_j) = \chi_i(\sigma_i)\chi_j(\sigma_j)$$

where (σ_i,σ_j) equals $(+1,+1)$, $(+1,0)$, $(0,+1)$, $(0,0)$, $(+1,-1)$, $(-1,+1)$, $(-1,-1)$, $(0,-1)$ and $(-1,0)$ when $n = 1,\ldots,9$, respectively. These may be rearranged into linear

combinations corresponding to eigenvalues of the total spin S. Hence, $\chi_S(\sigma_i, \sigma_j)$ can either be one of the $S_z = +2, +1, 0, -1, -2$ ($S = 2$) quintuplet states

$$\chi_S(\sigma_i, \sigma_j) = \begin{cases} \chi^{(1)}(\sigma_i, \sigma_j) \\ \frac{1}{\sqrt{2}}\chi^{(2)}(\sigma_i, \sigma_j) + \frac{1}{\sqrt{2}}\chi^{(3)}(\sigma_i, \sigma_j) \\ \frac{1}{\sqrt{2}}\chi^{(5)}(\sigma_i, \sigma_j) + \frac{1}{\sqrt{2}}\chi^{(6)}(\sigma_i, \sigma_j) \\ \frac{1}{\sqrt{2}}\chi^{(8)}(\sigma_i, \sigma_j) + \frac{1}{\sqrt{2}}\chi^{(9)}(\sigma_i, \sigma_j) \\ \chi^{(7)}(\sigma_i, \sigma_j) \end{cases} \tag{11}$$

or it can be one of the $S_z = +1, 0, -1$ ($S = 1$) triplet states

$$\chi_S(\sigma_i, \sigma_j) = \begin{cases} \frac{1}{\sqrt{2}}\chi^{(2)}(\sigma_i, \sigma_j) - \frac{1}{\sqrt{2}}\chi^{(3)}(\sigma_i, \sigma_j) \\ \frac{1}{\sqrt{2}}\chi^{(5)}(\sigma_i, \sigma_j) - \frac{1}{\sqrt{2}}\chi^{(6)}(\sigma_i, \sigma_j) \\ \frac{1}{\sqrt{2}}\chi^{(8)}(\sigma_i, \sigma_j) - \frac{1}{\sqrt{2}}\chi^{(9)}(\sigma_i, \sigma_j) \end{cases} \tag{12}$$

or, finally, the $S_z = 0$ ($S = 0$) singlet state

$$\chi_S(\sigma_i, \sigma_j) = \chi^{(4)}(\sigma_i, \sigma_j). \tag{13}$$

An interchange of σ_i and σ_j now makes the quintuplet and singlet states symmetric and the triplet state antisymmetric. Hence, equation (10) becomes

$$\phi(\boldsymbol{r}, \sigma) = [\exp(\mathrm{i}\boldsymbol{k}\cdot\boldsymbol{r}) - (-1)^S \exp(-\mathrm{i}\boldsymbol{k}\cdot\boldsymbol{r})]\chi^{(n)}(\sigma_i, \sigma_j).$$

The correct antisymmetry requires the $S = 1$ triplet for even L and the $S = 0$ singlet or the $S = 2$ quintuplet for odd L. Due to weak correlations in higher-L states, $L = 0$ and $L = 1$ are assumed in the two cases, respectively.

For the first term C_1 in the energy expansion, Ψ_1 is a normalized plane wave and H_1 is simply taken to be the kinetic energy operator

$$H_1 = -\frac{\hbar^2}{2m}\frac{\partial^2}{\partial r^2}.$$

For the second term C_2, the matrix elements of

$$H_2 = -\frac{\hbar^2}{4m}\left(\frac{\partial^2}{\partial R^2}\right) - \frac{\hbar^2}{m}\left(\frac{\partial^2}{\partial r^2}\right) + v(r)$$

are taken with respect to the Lth-wave contributions of Ψ_2, i.e., $\Psi_2^L = f_L \mathcal{P}_L \Phi_2$. The terms C_3, C_4, ... are discarded, and, using $J_L(kr) \equiv krj_L(kr)$ for the spherical Bessel equation, $E = E_1 + E_2$ becomes

$$E = \sum_{1\leqslant i\leqslant N}\frac{\hbar^2 k_i^2}{2m} + \sum\sum_{1\leqslant i<j\leqslant N}\frac{1}{\langle\Psi_2|\Psi_2\rangle}\sum_{L=0}^{\infty}\langle\Phi_2^L|v_L|\Phi_2^L\rangle \tag{14}$$

where the effective interaction is

$$v_L(r) = \begin{cases} -\lambda_L f_L^2(r) & r < d \\ v(r) & r > d \end{cases} \tag{15}$$

and

$$\langle\Psi_2|\Psi_2\rangle = 2\sum_{S=0}^{2}\left(\sum_{\{S_z\}}\left|\chi_S(\sigma_i,\sigma_j)\right|^2\right) \tag{16}$$

is obtained for the normalization of the wave function. Due to spherical symmetry, a radial variation results for $\delta E = 0$, i.e.,

$$\delta\int_0^d J_L^2\left[-\frac{\hbar^2}{m}\left(f_L''f_L + 2f_L'\frac{J_L'}{J_L}f_L\right) + (v+\lambda_L)f_L^2\right]\mathrm{d}r = 0 \tag{17}$$

where the explicit dependency on k has been eliminated by the choice of an average momentum. Using the root mean square value of $k \equiv |\frac{1}{2}(\boldsymbol{k}_i - \boldsymbol{k}_j)|$, the angular integration of $K = |\boldsymbol{k}_1 + \boldsymbol{k}_2|$ with respect to the geometry of allowed combinations for $\boldsymbol{k}_i, \boldsymbol{k}_j$ in (17) is

$$\int \mathrm{d}\Omega_K = \begin{cases} 4\pi & 0 < \frac{1}{2}K < k_\mathrm{F} - k \\ 4\pi\left(k_\mathrm{F}^2 - k^2 - \frac{1}{4}K^2\right)(kK)^{-1} & k_\mathrm{F} - k < \frac{1}{2}K < (k_\mathrm{F}^2 - k^2)^{1/2} \\ 0 & (k_\mathrm{F}^2 - k^2)^{1/2} < \frac{1}{2}K < \infty. \end{cases}$$

The total integration with respect to K of a pair of particles with a given k then becomes

$$\int \mathrm{d}^3K = \frac{32}{3}\pi k_\mathrm{F}^3\left[1 - \frac{3}{2}\left(\frac{k}{k_\mathrm{F}}\right) + \frac{1}{2}\left(\frac{k}{k_\mathrm{F}}\right)^3\right] \tag{18}$$

where k_F denotes the Fermi wavenumber. Thus,

$$k_{av} = \sqrt{0.3}k_\mathrm{F}$$

is obtained for the average momentum. Agreement with the boundary conditions introduces a constraint and requires the inclusion of a Lagrange multiplier λ_L. Hence, using $u_L(r) \equiv f_L(r)J_L(kr)$, equation (9) implies

$$u_L''(r) - \left\{\frac{m}{\hbar^2}\left[v(r) + \lambda_L\right] + \frac{L(L+1)}{r^2} - k_{av}^2\right\}u_L(r) = 0 \tag{19}$$

upon solution of the Euler–Lagrange equations. The Lagrange multiplier is thus the mathematical equivalent of our average background field.

The truncation (14) of the cluster expansion (6) is justified by the assumption that the most important contributions, i.e., those due to the core of the interaction, are of sufficiently short range to be described by two-body clustering terms (correlations with nearest neighbours only) and that all other contributions (the totality of interactions with distant neighbours as well as the intermediate- and long-range part of the nearest-neighbour interaction) are adequately described by the average field. It is important to realize the implication that correlations in the clustering sense are not present between distant neighbours in this assumption. Unfortunately, due to this truncation, the upper-bound variational property of (2) is lost in our calculations.

In conventional LOCV calculations, the conditions of healing are derived by requiring, on average, that the sum with respect to i and j over

$$P_2 = \frac{\langle\Psi_2|O_2|\Psi_2\rangle}{\langle\Psi_2|\Psi_2\rangle} \tag{20}$$

where

$$O_2 = \begin{cases} 0 & r > d \\ 1 & r < d \end{cases}$$

should be consistent with finding exactly one other particle within the correlation volume. For the $r < d$ probability per pair, this gives $P_2 = \overline{O}_2$, where

$$\overline{O}_2 = \frac{1}{N-1} \approx \frac{1}{N}$$

in the limit $N \to \infty$ of a large system. For a homogeneous isotropic system, this probability must be proportional to the probability per unit volume, i.e.,

$$P_2 = \zeta \frac{\omega(d)}{\Omega} \tag{21}$$

where ζ is the proportionality constant. We thus obtain

$$\rho\omega(d) = 1 \tag{22}$$

when $\zeta = 1$, for the healing conditions.

Equations (20) to (22) correspond to Pandharipande's original definition of the healing distance [13], where it is hoped that local correlations left out in the truncation of (6) are either sufficiently weak to be neglected or may be merged, without inducing too large errors, with the global-type correlations assumed for $f_L(r)$.

This may not represent the best choice of a healing distance, however, since the flexibility inherent in such a concept has then not been fully exploited. Using instead Nosanow's full expansion for the clustering probability, i.e.,

$$P = \frac{\langle \Psi | O | \Psi \rangle}{\langle \Psi | \Psi \rangle}$$

a separate treatment of local and global average contributions can be visualized by invoking an independent-particle-model analogy for the lowest-order terms in the series. In the expansion for E these terms represent the kinetic energy contributions, whereas in the expansion for P we define

$$P_1 = \binom{N}{1}^{-1} \sum_{1 \leqslant k \leqslant N} \langle O_1 \rangle$$

where $\langle O_1 \rangle$ is the normalized expectation value with respect to Ψ_1 of identifying particle i within some set n_i of particles, i.e.,

$$\langle O_1 \rangle \equiv \frac{\langle \Psi_1 | O_1 | \Psi_1 \rangle}{\langle \Psi_1 | \Psi_1 \rangle}.$$

Statistically, we obtain $P_1 = \overline{O}_1$, where

$$\frac{1}{N} \leqslant \overline{O}_1 \leqslant 1 \tag{23}$$

when $1 \leqslant n_i \leqslant N$, respectively. With a truncation of

$$P = \sum_{k=1}^{N} P_k \tag{24}$$

at $k = 1$, $P = 1$ requires $n_i = N$, in which case contributions are from the kinetic energy alone. Thus, the ideal gas provides an adequate model, $N = 1$ representing a free particle. Considering the $N > 1$ interacting system, on the other hand, we have $n_i < N$ for the number of uncorrelated particles, i.e., $P < 1$, a situation which may be interpreted as requiring an average field $\lambda_L^{(1)}$ for a 'full' description.

In the presence of strong short-range correlations, however, a specific treatment is required to handle local distortions to the field $\lambda_L^{(1)}$. We then consider in detail the correlations of i with j. Hence, setting $n_i = 1$, equation (23) is 're-scaled' to

$$\frac{1}{N(N-1)} \leqslant \overline{O}_1 \leqslant \frac{1}{N}$$

for the respective limits, when $1 \leqslant n_j \leqslant N-1$, on the joint probability of n_i and n_j. For the second-order term in Nosanow's cluster expansion,

$$P_2 = \binom{N}{2}^{-1} \sum \sum_{1 \leqslant i < j \leqslant N} \left\{ \langle O_2 \rangle - \binom{2}{1}^{-1} \sum_{i \leqslant k \leqslant j} \langle O_1 \rangle \right\} \tag{25}$$

we next introduce

$$O_2 = \begin{cases} \overline{O}_1 & r > \delta \\ 1 & r < \delta \end{cases}$$

where $\langle O_2 \rangle$ is the expectation value with respect to Ψ_2 of observing $r < \delta$. Defining

$$\widetilde{O}_2 \equiv \overline{O_2 - \overline{O}_1} \tag{26}$$

we obtain statistically $P_2 = \widetilde{O}_2$, and (26) becomes

$$\widetilde{O}_2 = \frac{\widehat{\eta} N - n_j}{N(N-1)}$$

$\widehat{\eta}$ being the number of times that $r < \delta$ occurs in the expansion with respect to i. For each sum over j, the occurrence of a single such event, i.e., $\widehat{\eta} = 1$, constitutes two-body clustering. Considering $N = 2$, we have $n_j = 1$, and since

$$P = \frac{n_j(N-2) + \widehat{\eta} N}{N(N-1)} \tag{27}$$

the only solution which is consistent with $P = 1$ is $\widehat{\eta} = 1$. This corresponds to two-body scattering. Considering $N = 3$, on the other hand, we have $1 \leqslant n_j \leqslant 2$. In this case, $P = 1$ requires

$$\frac{4}{3} \leqslant \widehat{\eta} \leqslant \frac{5}{3}.$$

That is, it requires cluster contributions beyond second order. Assuming $\widehat{\eta} = 1$ nonetheless, we obtain for the clustering probability

$$\frac{2}{3} \leqslant P \leqslant \frac{5}{6}$$

i.e., $P < 1$, and a local clustering field $\lambda_L^{(2)}$ must be used to account for the truncation of (24) at $k = 2$. From (27) we see that $P = 1$ can also be obtained with $\widehat{\eta} = 1$ for *any* value of N, provided that $n_j = N$. However, $n_j = N$ would mean that the independent-particle model provides an adequate description. Hence, $\widetilde{O}_2$ vanishes, as it should for a weakly interacting system. For $N > 1$, we generally obtain

$$\frac{1}{N(N-1)} \leqslant \widetilde{O}_2 \leqslant \frac{1}{N}$$

when $N - 1 \geqslant n_j \geqslant 1$. With

$$P_2 = \frac{\omega(\delta)}{\Omega}$$

this leads to

$$\frac{1}{N-1} \leqslant \rho\omega(\delta) \leqslant 1 \tag{28}$$

where $N > 1$, for the healing condition.

It may be noted that, consistently with the truncation at $n = 2$ of the expansion for E, equation (22) is now obtained for $N = 2$ rather than in the limit $N \to \infty$. Thus, for $N \geqslant 2$, the parameter ζ in (21) can be stated as

$$0 < \zeta \leqslant 1$$

providing a 'renormalized' healing condition, i.e., $\omega(d) \to \omega(\delta) = \zeta\omega(d)$, whereby a modified healing distance $\delta < d$ is obtained for $\zeta < 1$. As ζ is decreased within the interval above, the validity of (28) becomes more questionable. The average field λ_L may thus, in general, be regarded as a compromise between a global long-range attractive field and a local short-range repulsive 'clustering' field.

Next, the sum over distinct pairs i, j is replaced by an integration; that is, for some function G we obtain

$$\frac{1}{2}\sum_{k_i \neq k_j}^{k_N}\sum^{k_N} G(k_i, k_j) \to \frac{1}{2}\eta^2 \int_{|\boldsymbol{k}|<k_F} G(k) \int \mathrm{d}^3K\ \mathrm{d}^3k \tag{29}$$

where

$$\eta = \nu\frac{\Omega}{(2\pi)^3}$$

is the density of states in the Fermi sea, and (18) represents the centre-of-mass integration. Equation (29), in combination with

$$\int \Big[1 \pm \cos(2\boldsymbol{k}\cdot\boldsymbol{r})\Big] \int \mathrm{d}^3K\ \mathrm{d}^3k = \frac{16}{9}\pi^2 k_F^6[1 \pm S^2(k_F r)]$$

where

$$S(k_F r) \equiv \frac{3}{k_F^3 r^3}[\sin(k_F r) - (k_F r)\cos(k_F r)]$$

is the Slater function, determines the average contribution to P_2 from the matrix element $\langle O_2\rangle$ in (25). Defining

$$F_L(k_F r) = 1 + (-1)^L S^2(k_F r)$$

we obtain

$$\omega(\delta) = 4\pi\sum_{L=0}^{1}\alpha_L\omega_L(\delta) \tag{30}$$

where we have

$$\omega_L(\delta) = \int_0^\delta f_L^2(r)F_L(k_F r)r^2\ \mathrm{d}r \tag{31}$$

with the parameters α_0 and α_1 depending on the spin states (11), (12) and (13). For $\nu = 1$, spins occur in the $\{+1\}$, $\{0\}$ or $\{-1\}$ state. Hence, the spin function is a quintuplet or a singlet state and we obtain $\alpha_0 = 0$ and $\alpha_1 = 1$. For $\nu = 2$, spins are evenly distributed over the $\{+1, -1\}$, $\{+1, 0\}$ and $\{0, -1\}$ states. Whereas all three cases then involve one triplet contribution, $\{+1, 0\}$ and $\{0, -1\}$ additionally involve two quintuplet contributions and a singlet contribution. Three additional quintuplet contributions are involved for $\{+1, -1\}$, but no singlet contribution in this case. The result for $\nu = 2$, then, in all three cases, is $\alpha_0 = \frac{1}{4}$ and $\alpha_1 = \frac{3}{4}$. Finally, for $\nu = 3$,

spins are distributed evenly over the $\{+1, 0, -1\}$ states. Hence, all singlet, triplet and quintuplet states contribute, in which case we obtain $\alpha_0 = \frac{1}{3}$ and $\alpha_1 = \frac{2}{3}$.

The ground-state energy per particle, $\mathcal{E} = E/N$, is now obtained from the truncated energy expansion (14). An integration over the Fermi sea gives

$$k_{\mathrm{F}}^3 = \frac{6\pi^2\rho}{\nu}$$

and hence the kinetic energy per particle is obtained as

$$\mathcal{E}_1 = \frac{3\hbar^2 k_{\mathrm{F}}^2}{10m}. \tag{32}$$

Using (14), (15), (16), (29) and (31), we obtain for the potential interaction energy per particle

$$\mathcal{E}_2 = -2\pi\rho \sum_{L=0}^{1} \alpha_L \left[\lambda_L \omega_L(\delta) - \int_{\delta}^{\infty} v(r) F_L(k_{\mathrm{F}} r) r^2 \, \mathrm{d}r \right]. \tag{33}$$

Finally, with (32) and (33), the total energy reads

$$\mathcal{E} = \mathcal{E}_1 + \mathcal{E}_2. \tag{34}$$

3. Results

The results of our LOCV calculations are obtained by solving (19), (30) and (34) self-consistently with respect to the boundary conditions on $f_L(r)$, i.e., equation (9). Below, results corresponding to density increments of 10^{-4} Å^{-3} are displayed.

For conventional LOCV calculations, using $\zeta = 1$ in (21), energy minima for the three phases obtained with the S1, S2 and LJ interaction models are included in table 1, and curves for $\mathcal{E}(\rho)$ obtained with the S2 interaction model are displayed in figure 1. The only potential which gives negative energy minima in all phases is the LJ model. The S1 and S2 results are negative for the $\downarrow\mathrm{D}_2^{\uparrow}$ and $\downarrow\mathrm{D}_3^{\uparrow}$ phases only. Generally, the difference in energy between $\nu = 3$ and $\nu = 2$ is seen to be somewhat less than half the difference between $\nu = 2$ and $\nu = 1$. Furthermore, results obtained with the S2 model are 0.25–0.3 K lower than the S1 results, and results obtained with the LJ model approximately 0.5 K lower than the S2 results. An increase of about 12% is observed in the equilibrium density ρ_0 as the spin degeneracy increases from $\nu = 1$ to $\nu = 2$. Between $\nu = 2$ and $\nu = 3$, however, the equilibrium densities increase by a much smaller amount. The results which agree best with the VMC results are those obtained with the S1 interaction model. There are no inversions, i.e., the correct ordering $\mathcal{E}(\downarrow\mathrm{D}_3^{\uparrow}) < \mathcal{E}(\downarrow\mathrm{D}_2^{\uparrow}) < \mathcal{E}(\downarrow\mathrm{D}_1^{\uparrow})$ is also obtained for the energy levels.

Table 1. Ground-state energy minima for the $\downarrow\mathrm{D}_1^{\uparrow}$, $\downarrow\mathrm{D}_2^{\uparrow}$ and $\downarrow\mathrm{D}_3^{\uparrow}$ phases obtained in conventional LOCV calculations ($\zeta = 1$) with the S1, S2 and LJ potentials.

	$\nu = 1$		$\nu = 2$		$\nu = 3$	
	ρ_0 (Å^{-3})	$\mathcal{E}$ (K)	ρ_0 (Å^{-3})	$\mathcal{E}$ (K)	ρ_0 (Å^{-3})	$\mathcal{E}$ (K)
S1	0.00425	0.312	0.00478	−0.040	0.00476	−0.209
S2	0.00468	0.051	0.00524	−0.332	0.00522	−0.499
LJ	0.00499	−0.417	0.00564	−0.845	0.00566	−1.005

In modified LOCV calculations, equation (28) is applied in a mode corresponding to $N > 2$. A decrease is then observed in λ with ρ, indicating that cluster contributions neglected in the truncation of (6) are mainly of a repulsive nature. As far as the two-body interaction is

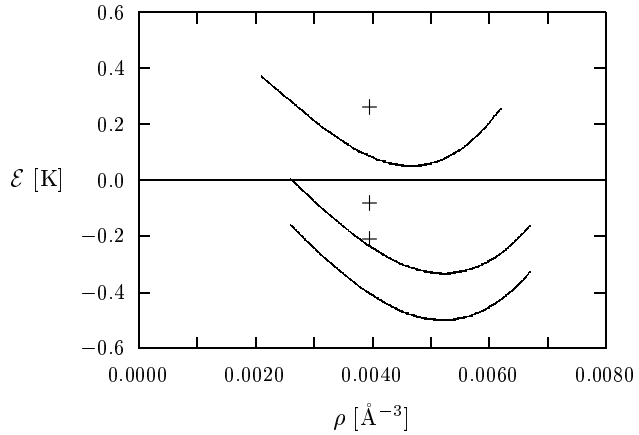

Figure 1. Conventional LOCV results ($\zeta = 1$) obtained with the S2 model for the $\downarrow D_1^{\uparrow}$, $\downarrow D_2^{\uparrow}$ and $\downarrow D_3^{\uparrow}$ phases, and the VMC minima (+). Both the LOCV and VMC results shown have $\mathcal{E}(\downarrow D_3^{\uparrow}) < \mathcal{E}(\downarrow D_2^{\uparrow}) < \mathcal{E}(\downarrow D_1^{\uparrow})$.

concerned, the repulsive core thus increases in relative importance. Moreover, modifications are restricted to $L = 1$ interactions, since effects of higher-order clustering should be less likely in $L = 0$ central-force interactions.

The equilibrium density reported in the VMC calculations is the same in all three phases, i.e., 0.0040 Å^{-3}. Considering bulk $\downarrow D_1^{\uparrow}$, the modified LOCV energy minimum consistent with this density, using $\zeta_1 = 0.931$, is +0.146 K. Comparing instead with the ground-state energy reported in VMC calculations, i.e., +0.26 K, an equilibrium density of 0.0027 Å^{-3} is obtained for $\zeta_1 = 0.775$. A value which passes through the VMC minimum is obtained for $\zeta_1 = 0.856$, the modified LOCV minimum of 0.217 K in this case occurring at a density of 0.0033 Å^{-3}. An overall 'best fit' is suggested in figure 2 where the minimum of $\mathcal{E} = 0.186$ K is obtained at $\rho_0 = 0.0036$ Å^{-3}, using $\zeta_1 = 0.893$. Numerical values for $\mathcal{E}(\rho)$ corresponding to the results

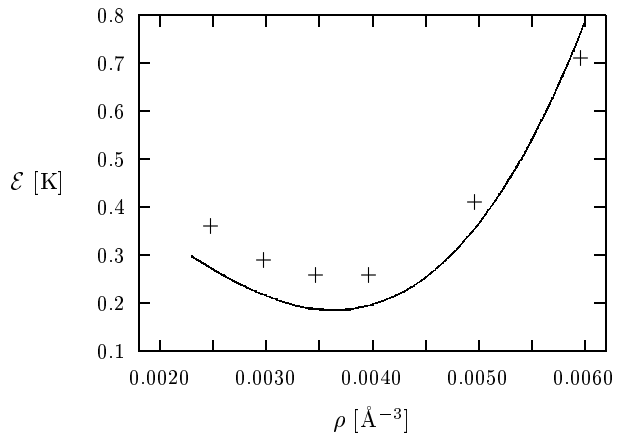

Figure 2. The ground-state energy $\mathcal{E}(\rho)$ for the $\downarrow D_1^{\uparrow}$ phase, where modified S2 LOCV results (solid line: $\zeta_1 = 0.893$) and VMC (+) results are compared.

displayed in figure 2 are included in table 2, where data for the average field λ_1 and the healing distance δ are also included. The decrease obtained in λ_1 when ζ_1 is reduced to 0.893 varies between 0.13 K at 0.0025 Å^{-3} and 1.92 K at 0.0060 Å^{-3}, being 0.65 K at 0.0040 Å^{-3}. The corresponding decrease in δ, which is about 0.11 Å at 0.0040 Å^{-3}, is approximately constant for this range of densities.

Table 2. Results for the $\downarrow D_1^{\uparrow}$ phase obtained in modified LOCV calculations with the S2 model for the two-body interactions.

	VMC[a]	Modified LOCV[b]				
ρ (Å^{-3})	$\mathcal{E}$ (K)	δ (Å)	δ/ρ	λ_0 (K)	λ_1 (K)	$\mathcal{E}$ (K)
0.0025	0.36	5.569	1.234	—	0.580	0.271
0.0030	0.29	5.308	1.249	—	0.037	0.216
0.0035	0.26	5.101	1.262	—	−0.750	0.188
0.0040	0.26	4.931	1.274	—	−1.780	0.197
0.0045		4.787	1.285	—	−3.053	0.253
0.0050	0.41	4.663	1.296	—	−4.565	0.364
0.0055		4.554	1.306	—	−6.315	0.538
0.0060	0.71	4.457	1.315	—	−8.298	0.782

[a] Variational Monte Carlo results, from reference [8].
[b] Using (28), with $\zeta_1 = 0.893$.

For the $\downarrow D_2^{\uparrow}$ phase, the energy minimum consistent with equilibrium at 0.0040 Å^{-3} is −0.148 K, and is obtained for $\zeta_1 = 0.839$. The result obtained for $\zeta_1 = 0.788$, however, corresponds to an energy minimum of −0.106 K at 0.0036 Å^{-3}, and seems to fit the VMC values over the entire range of densities reported rather well. The result is shown in figure 3. The changes in λ_0, λ_1 and δ with ζ_1 and ρ are analogous to those in the $\downarrow D_1^{\uparrow}$ phase, with decreases of 1.39 K, 0.87 K and 0.16 Å, respectively, being obtained at 0.0040 Å^{-3}. Numerical data for some of the densities in the result displayed are included in table 3.

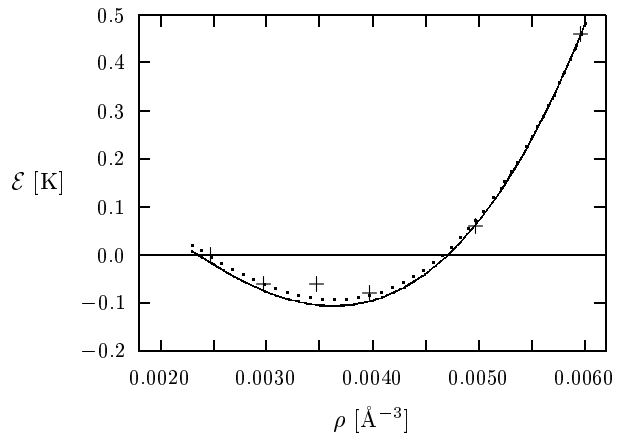

Figure 3. The ground-state energy $\mathcal{E}(\rho)$ for the $\downarrow D_2^{\uparrow}$ phase, where modified S2 LOCV results (solid line: $\zeta_0 = 1$, $\zeta_1 = 0.788$; dotted line: $\zeta_0 = 0.980$, $\zeta_1 = 0.800$) and VMC (+) results are compared.

The $\downarrow D_3^{\uparrow}$ phase result consistent with the VMC density of 0.0040 Å^{-3} is −0.314 K, and is obtained for $\zeta_1 = 0.801$. Consistency with the VMC energy, on the other hand, moves the

Table 3. Results for the $\downarrow D_2^{\uparrow}$ phase obtained in modified LOCV calculations with the S2 model for the two-body interactions.

	VMC[a]	Modified LOCV[b]				
ρ (Å^{-3})	$\mathcal{E}$ (K)	δ (Å)	δ/ρ	λ_0 (K)	λ_1 (K)	$\mathcal{E}$ (K)
0.0025	0.00	5.526	1.226	−2.078	0.727	−0.019
0.0030	−0.06	5.275	1.242	−3.230	0.230	−0.076
0.0035	−0.06	5.075	1.256	−4.619	−0.501	−0.105
0.0040	−0.08	4.910	1.269	−6.243	−1.466	−0.096
0.0045		4.770	1.281	−8.102	−2.664	−0.040
0.0050	0.06	4.649	1.293	−10.19	−4.093	0.069
0.0055		4.543	1.303	−12.51	−5.752	0.240
0.0060	0.46	4.448	1.313	−15.05	−7.637	0.478

[a] Variational Monte Carlo results, from reference [8].
[b] Using (28), with $\zeta_1 = 0.788$.

equilibrium density as far down as 0.0030 Å^{-3}, in which case $\zeta_1 = 0.635$. With $\zeta_1 = 0.740$, a more successful fit between modified LOCV values and VMC benchmarks is obtained, the ground-state energy and equilibrium density in this case being −0.270 K and 0.0036 Å^{-3}, respectively. The result is shown in figure 4. Corresponding numerical values are included in table 4, and the observed decreases in λ_0, λ_1 and δ with ζ_1 at 0.0040 Å^{-3} are 1.02 K, 0.66 K and 0.12 Å, respectively.

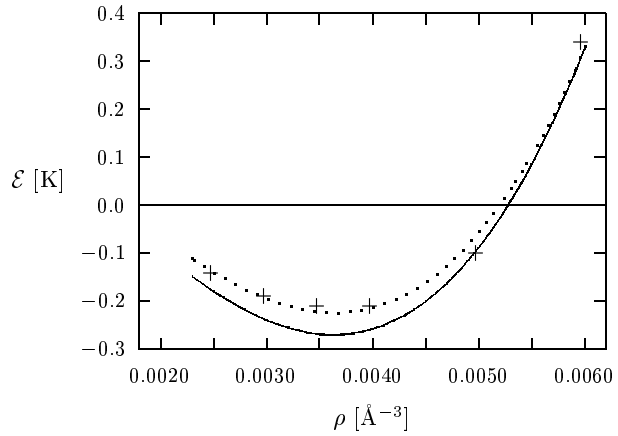

Figure 4. The ground-state energy $\mathcal{E}(\rho)$ for the $\downarrow D_3^{\uparrow}$ phase, where modified S2 LOCV results (solid line: $\zeta_0 = 1$, $\zeta_1 = 0.740$; dotted line: $\zeta_0 = 0.950$, $\zeta_1 = 0.796$) and VMC (+) results are compared.

Plots of the effective interactions (15) are included in figure 5 and figure 6, where the density dependencies of $v_0(r)$ and $v_1(r)$ are shown for the values of ρ that have been included in the tables.

4. Discussion

In comparing with VMC benchmarks, a few remarks should be made about some of the approximations used in the LOCV method. Triplet correlations in VMC calculations are

Table 4. Results for the $\downarrow D_3^{\uparrow}$ phase obtained in modified LOCV calculations with the S2 model for the two-body interactions.

	VMC[a]	Modified LOCV[b]				
ρ (Å^{-3})	$\mathcal{E}$ (K)	δ (Å)	δ/ρ	λ_0 (K)	λ_1 (K)	$\mathcal{E}$ (K)
0.0025	−0.14	5.493	1.220	−1.931	0.763	−0.178
0.0030	−0.19	5.248	1.237	−3.041	0.266	−0.239
0.0035	−0.21	5.052	1.251	−4.384	−0.464	−0.268
0.0040	−0.21	4.890	1.265	−5.958	−1.425	−0.259
0.0045		4.753	1.277	−7.761	−2.618	−0.201
0.0050	−0.10	4.634	1.289	−9.790	−4.038	−0.089
0.0055		4.530	1.300	−12.04	−5.685	0.084
0.0060	0.34	4.437	1.310	−14.52	−7.555	0.325

[a] Variational Monte Carlo results, from reference [8].
[b] Using (28), with $\zeta_1 = 0.740$.

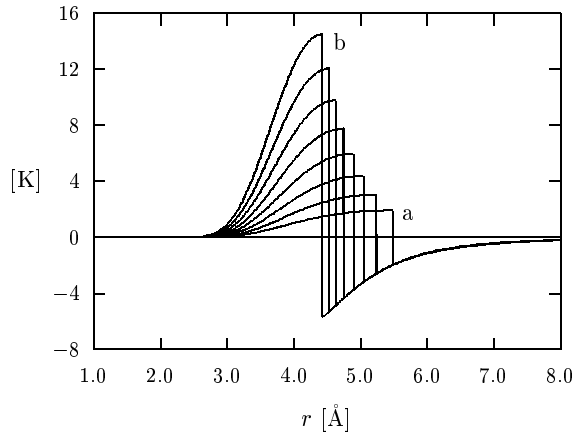

Figure 5. The $L = 0$ effective interaction (15) obtained for the $\downarrow D_3^{\uparrow}$ phase, with ρ varied in steps of 0.0005 Å^{-3} between (a) 0.0025 Å^{-3} and (b) 0.0060 Å^{-3}.

explicitly incorporated into the wave function by generalizing upon the Jastrow *ansatz*; provided that the most important correlations are between nearest neighbours only, Jastrow correlations defined in conjunction with an average field should not give results that are radically different from this prescription. Also, whereas an explicit momentum dependence is built into the wave function in VMC calculations [17], the momentum is treated in an average way in LOCV calculations. Nevertheless, for Fermi systems intermediate in coupling strength between nuclear matter and liquid ^{3}He, an average over allowed momentum states in the Fermi sea is expected to be a good approximation [18]. Due to the truncation of the cluster expansion, however, the feature which is most likely to affect comparisons with VMC results is the loss of the upper-bound variational property. This results in the ground-state energy levels being systematically underestimated, an effect which is accentuated for strongly coupled systems and in the presence of significant short-range correlations beyond nearest neighbours. The characteristic underestimation is clearly visible in figure 1, where LOCV levels are seen to be consistently lower than VMC levels.

A number of methods have been used in calculations for many-body $\downarrow D_{\nu}^{\uparrow}$. The result

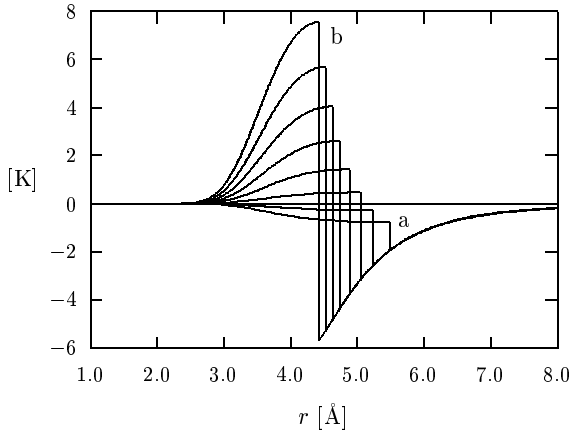

Figure 6. The $L = 1$ effective interaction (15) obtained for the $\downarrow D_3^{\uparrow}$ phase, with ρ varied in steps of 0.0005 Å^{-3} between (a) 0.0025 Å^{-3} and (b) 0.0060 Å^{-3}.

obtained for the $\downarrow D_1^{\uparrow}$ phase with a Galitskii–Feynman–Hartree–Fock (GFHF) method, using the S2 interaction model, is +41 K at 0.0034 Å^{-3} [19]. Fermi hypernetted-chain techniques [20] in conjunction with correlated basis functions [21] have also been applied. Although the latter FHNC–CBF scheme is generally regarded as more reliable than the GFHF method, the delicate balance between kinetic and potential energy contributions is in this case obscured by statistical errors.

The result obtained for bulk $\downarrow D_1^{\uparrow}$ with the FHNC–CBF approach is +0.26 K at 0.0040 Å^{-3} [21]. In the VMC benchmark calculations, conclusions drawn from the FHNC–CBF scheme were used to obtain a trial wave function which improves upon the basic two-body Jastrow form by including triplet and momentum-dependent correlations. In the $\downarrow D_1^{\uparrow}$ phase, however, the Jastrow energy alone was assumed to be sufficient in FHNC–CBF calculations. The effects of triplet and backflow correlations in VMC calculations are negligible in this case, but according to Panoff and Clark [8], the $\downarrow D_1^{\uparrow}$ phase result of +0.26 K at 0.0040 Å^{-3} should probably be lowered somewhat. Although the conventional S2 LOCV result obtained is 0.21 K lower, it still lies above the gas–liquid interphase. This is a very strong indication that bulk $\downarrow D_1^{\uparrow}$ should be a gas in the ground state, since the right-hand-side limit of (28) represents a 'lower bound' for the energy in our calculations.

An interesting question related to results for the $\downarrow D_1^{\uparrow}$ phase is that of how well the Jastrow function describes the ground state of a spin-polarized Fermi system. For instance, for liquid ^{3}He the Jastrow function alone provides better results for the fully spin-polarized phase, the exclusion principle then being more effective in preventing a close proximity between particles. Specifically, in FHNC calculations for liquid ^{3}He, inclusion of triplet correlations and backflow amounts to a shift in the ground-state energy of -0.24 K for the fully spin-polarized phase and -1.08 K for the unpolarized phase [7]. The corresponding discrepancies between FHNC results and conventional LOCV results increase from as little as 0.2 K in the former case to 0.7 K in the latter case [5]. In the present calculations the discrepancies between VMC and LOCV results are more or less comparable, i.e., $\Delta\mathcal{E}(\downarrow D_1^{\uparrow}) = 0.21$ K, $\Delta\mathcal{E}(\downarrow D_2^{\uparrow}) = 0.25$ K and $\Delta\mathcal{E}(\downarrow D_3^{\uparrow}) = 0.29$ K, where $\Delta\mathcal{E} \equiv \mathcal{E}_{\rm VMC} - \mathcal{E}_{\rm LOCV}$. A lowering of the Jastrow energy by $\sim$0.05–0.10 K, however, would enable a more precise fit to be obtained for the modified LOCV results to the VMC results. Also, the LOCV Jastrow discrepancy would be notably less in the

$\downarrow D_1^{\uparrow}$ phase than in both the $\downarrow D_2^{\uparrow}$ and $\downarrow D_3^{\uparrow}$ phases.

For the $\downarrow D_2^{\uparrow}$ phase, a CBF perturbative correction of -0.23 K is obtained in FHNC–CBF calculations. This results in a ground-state energy of +0.05 K at 0.0035 Å^{-3} [21]. The S2 GFHF result in this case is +0.03 K at 0.0032 Å^{-3} [19]. With triplet and backflow correlations, Panoff and Clark obtain the benchmark saturation value for the $\downarrow D_2^{\uparrow}$ system, i.e., -0.08 K at 0.0040 Å^{-3} [8]. The result which saturates at the VMC energy minimum in modified LOCV calculations, on the other hand, is obtained at 0.0034 Å^{-3} for $\zeta_1 = 0.750$. In this case, no healing condition (28) with modifications to the $L = 1$ interaction component is consistent with a result in the gas phase. That is, when ζ_1 is reduced, the saturation value initially moves more or less linearly towards higher energies and lower densities. As the gas–liquid interphase is approached, a (negative) maximum is reached, whereupon the minimum again moves downward. Only when modifications to the $L = 0$ interaction component are included is saturation possible in the gaseous phase. It should, however, be remembered that the conditions of healing increasingly become more questionable as one moves further away from the right-hand side limit of (28). Nevertheless, our LOCV results are still a very good indication that bulk $\downarrow D_2^{\uparrow}$ should be a self-bound liquid.

The CBF perturbative correction reported for the $\downarrow D_3^{\uparrow}$ phase in FHNC–CBF calculations is -0.27 K, the ground-state energy now being -0.15 K at 0.0035 Å^{-3} [21]. The energy obtained in S2 GFHF calculations is -0.31 K at 0.0035 Å^{-3} [19]. Hence, reliable results obtained for this system are all consistent with a ground-state energy below the liquid–gas interphase, Panoff and Clark's benchmark value being -0.21 K at 0.0040 Å^{-3}. The gaseous phase is highly improbable, since in our calculations the $\nu = 3$ energy always occurs below the $\nu = 2$ energy. In fact, this system is bound already at the two-body Jastrow level in VMC calculations [22].

The results shown in figures 2, 3 and 4 all saturate at a density of 0.0036 Å^{-3} with the healing conditions chosen. In the case of the $\downarrow D_1^{\uparrow}$ phase, however, the exact position of the minimum is uncertain and the 'best fit' shown was chosen so as to agree with the saturation densities of the other two phases. As far as liquid ^{3}He is concerned, triplet contributions obtained in VMC calculations are seen to be almost exclusively due to the $L = 1$ interaction component [23]. The decrease observed in the parameter ζ_1 is somewhat larger than that obtained for the healing conditions of liquid ^{3}He [5]. Thus, to see how higher-order correlations in the central-force component might affect the energy, the minimum obtained by modifying the $L = 1$ component may be used as an initial approximation when modifications to $L = 0$ are considered. In the $\downarrow D_2^{\uparrow}$ phase, modifications to $L = 0$ should probably be small since the result already obtained for $\mathcal{E}(\rho)$ agrees very well with VMC values.

Thus, considering equilibrium densities in the range 0.0035 Å^{-3} to 0.0040 Å^{-3}, ζ_0 is gradually decreased while requiring ζ_1 to be consistent with the equilibrium density obtained when only $L = 1$ is modified. In figure 3, a result for $\mathcal{E}(\rho)$ is suggested which fits the VMC values over the range reported. Using $\zeta_0 = 0.980$ and $\zeta_1 = 0.800$, the equilibrium density obtained in this case is $\rho_0 = 0.003\,64$ Å^{-3} with a ground-state energy of $\mathcal{E} = -0.092$ K. For the $\downarrow D_3^{\uparrow}$ phase, an overall $\mathcal{E}(\rho)$ which fits the VMC values very well over the range reported also saturates at $\rho_0 = 0.003\,64$ Å^{-3}. This result, included in figure 4, is obtained with $\zeta_0 = 0.950$ and $\zeta_1 = 0.796$, the energy minimum now being $\mathcal{E} = -0.224$ K. That the bare two-body Jastrow formalism becomes less accurate when the polarization is decreased is also evident when the $\downarrow D_2^{\uparrow}$ and $\downarrow D_3^{\uparrow}$ phases are compared. Although apparently the decrease in ζ_1 is small, separate modifications to $L = 0$ and $L = 1$ seem to indicate that the $\downarrow D_3^{\uparrow}$ system is more correlated in the central-force component than the $\downarrow D_2^{\uparrow}$ system.

On the basis of the optimum fits obtained for LOCV results to benchmark VMC results,

it would thus seem that the $\downarrow D_2^{\uparrow}$ and $\downarrow D_3^{\uparrow}$ phases both saturate at the same value. We are, however, unable to determine with certainty whether or not the equilibrium density should be identical in the three phases, since this ultimately requires an independent way of quantifying the parameters ζ_0 and ζ_1. Nevertheless, when consistency is required in the ordering of energy levels between the $\downarrow D_1^{\uparrow}$, $\downarrow D_2^{\uparrow}$ and $\downarrow D_3^{\uparrow}$ phases, any significant variation in the density dependencies of other ground-state properties should become evident in modified LOCV calculations [24].

The behaviour of the energy with the density is also in agreement with the VMC results reported when the $\downarrow D_2^{\uparrow}$ and $\downarrow D_3^{\uparrow}$ phases are considered. The results which differ most from VMC results are again obtained for the $\downarrow D_1^{\uparrow}$ phase. Not only does $E(\rho)$ lie somewhat below the VMC values, but in LOCV calculations it is also steeper. This could be an indication that the elastic response of the fully polarized system should be 'stiffer' than that of more degenerate systems. When the compressibility is considered, the respective saturation values obtained for the $\downarrow D_1^{\uparrow}$, $\downarrow D_2^{\uparrow}$ and $\downarrow D_3^{\uparrow}$ phases are 0.937, 0.961 and 0.996 atm^{-1}. For the $\downarrow D_2^{\uparrow}$ and $\downarrow D_3^{\uparrow}$ phases these results correspond to LOCV calculations with both the $L = 0$ and $L = 1$ interaction components modified, i.e., those results which best fit the VMC values.

As to the nature of the phase diagram, no essentially new features emerge in our calculations. Although, for instance, the (unknown) dependency of ζ upon ρ should change with ν, it is unlikely that such a change should cause a reversal in the stability of the phases. The steeper $\downarrow D_1^{\uparrow}$ result obtained for $E(\rho)$ in our calculations more probably strengthens the case for a stable ordering.

5. Conclusions

To summarize, the constrained variational method provides a realistic description of ground-state many-body $\downarrow D_{\nu}^{\uparrow}$. Although the results for the ground-state energy are only 0.2–0.3 K below the VMC results, an effect which is due to the truncation of the cluster expansion, almost perfect agreement is obtained for the $\downarrow D_2^{\uparrow}$ and $\downarrow D_3^{\uparrow}$ phases when the healing condition is modified. Our results also definitely rule out the existence of bulk $\downarrow D_1^{\uparrow}$ in a liquid state. Modified LOCV estimates for this system generally lie somewhat lower than the VMC result, the conventional limit of the healing condition providing a 'lower bound' of +0.05 K. Our best estimate for the saturation densities of the $\downarrow D_2^{\uparrow}$ and $\downarrow D_3^{\uparrow}$ systems is 0.0036 Å^{-3}. This estimate, while not being inconsistent with the $\downarrow D_1^{\uparrow}$ phase, is less certain in this particular case. The energy of the $\downarrow D_1^{\uparrow}$ phase also increases more steeply with the density in our calculations.

References

[1] Stwalley W C and Nosanow L H 1976 *Phys. Rev. Lett.* **36** 910
[2] Skjetne B and Østgaard E 1996 *J. Low Temp. Phys.* **104** 275
[3] Skjetne B and Østgaard E 1998 *Int. J. Mod. Phys.* B **12** 2115
[4] Boronat J and Casulleras J 1994 *Phys. Rev.* B **49** 8920
[5] Skjetne B and Østgaard E 1998 *J. Low Temp. Phys.* **113** 55
[6] Moroni S, Fantoni S and Senatore G 1995 *Phys. Rev.* B **52** 13 547
[7] Manousakis E, Fantoni S, Pandharipande V R and Usmani Q N 1983 *Phys. Rev.* B **28** 3770
[8] Panoff R M and Clark J W 1987 *Phys. Rev.* B **36** 5527
[9] Kolos W and Wolniewicz L 1974 *Chem. Phys. Lett.* **24** 457
[10] Etters R D, Duang J V and Palmer R W 1975 *J. Chem. Phys.* **62** 313
[11] Silvera I F 1980 *Rev. Mod. Phys.* **52** 393
[12] Friend D G and Etters R D 1980 *J. Low Temp. Phys.* **39** 409
[13] Pandharipande V R 1971 *Nucl. Phys.* A **174** 641

[14] Van Kampen N G 1961 *Physica* **27** 783
[15] Nosanow L H 1966 *Phys. Rev.* **146** 120
[16] Jastrow R 1955 *Phys. Rev.* **98** 1479
[17] Schmidt K E, Lee M A, Kalos M H and Chester G V 1981 *Phys. Rev. Lett.* **47** 807
[18] Alexandrov I, Moszkowski S A and Wong C W 1975 *Nucl. Phys.* A **252** 13
[19] Greef C W, Clements B E, Talbot E F and Glyde H R 1990 *Phys. Rev.* B **43** 7595
[20] Krotscheck E, Smith R A, Clark J W and Panoff R M 1981 *Phys. Rev.* B **24** 6383
[21] Flynn M F, Clark J W, Krotscheck E, Smith R A and Panoff R M 1985 *Phys. Rev.* B **32** 2945
[22] Panoff R M, Clark J W, Lee M A, Schmidt K E, Kalos M H and Chester G V 1982 *Phys. Rev. Lett.* **48** 1675
[23] Moroni S, Fantoni S and Senatore G 1995 *Europhys. Lett.* **30** 93
[24] Skjetne B and Østgaard E 1998 *Nuovo Cimento* D **20** 811